Molecular Neurobiology (2019) 56:3404–3419
https://doi.org/10.1007/s12035-018-1307-2

# Plasmalogens Inhibit Endocytosis of Toll-like Receptor 4 to Attenuate the Inflammatory Signal in Microglial Cells

Fatma Ali[1] · Md. Shamim Hossain[2] · Sanyu Sejimo[3] · Koichi Akashi[3]

Received: 15 May 2018 / Accepted: 7 August 2018 / Published online: 20 August 2018


## Abstract

Microglial activation is a pathological feature of many neurodegenerative diseases and the role of cellular lipids in these diseases is mostly unknown. It was known that the special ether lipid plasmalogens (Pls) were reduced in the brain and blood samples of Alzheimer's disease (AD) patients. It has recently been reported that the oral ingestion of scallop-derived Pls (sPls) improved cognition among mild AD patients, which led us to investigate the role of sPls in the microglial activation. We used the lipopolysaccharides (LPS)-induced microglial activation model and found that sPls inhibit the LPS-mediated TLR4 endocytosis and the downstream caspases activation. By using the specific inhibitors, we also confirmed that the TLR4 endocytosis and the caspases activation strictly controlled the pro-inflammatory cytokine expression. In addition, the reduction of cellular Pls by sh-RNA-mediated knockdown of GNPAT (glyceronephosphate O-acyltransferase), a Pls synthesizing enzyme, enhanced the endocytosis of TLR4 and activation of caspase-3 which resulted in the enhanced pro-inflammatory cytokine expression. We also report for the first time that the TLR4 endocytosis was significantly higher in the cortex of aged mice and AD model mice brains, proposing a significant link between the age-related reduction of Pls and microglial activation. Interestingly, the sPls drinking in AD model mice significantly reduced the TLR4 endocytosis. Our cumulative data indicates that the cellular Pls attenuate the microglial activation by maintaining the endocytosis of TLR4, suggesting a possible mechanism of the cognition improvement effect of sPls among mild AD patients.

**Keywords** Endocytosis · Caspase-3 · TLR4 · Plasmalogens

## Introduction

Alzheimer disease (AD) is characterized by the progressive loss of neurons due to intracellular accumulation of toxic amyloid-β, as well as neuro-fibrillary tangles [1, 2]. Furthermore, the presence of activated microglia [3] and reactive astrocytes [4] that produce cytokines [5] are associated with the AD pathologies. Plasmalogens (Pls) are the member of glycerophospholipids containing a vinyl ether bond at the sn-1 position of the glycerol backbone [6]. This vinyl ether bond makes Pls more susceptible to oxidative stress than the sn-1 ester bond of diacylglycerophospholipids or carbon-carbon double bond of unsaturated fatty acids without producing free radicals in response to peroxides [7]. The deficiency of Pls has been found in the brain tissue [8–10] and serum samples [11] of AD patients. Pls have been shown to inhibit neuronal cell death by suppressing an intrinsic apoptotic pathway, which is characterized by the activation of caspase-9 [12]. It was also found that the systemic LPS-induced activation of microglial cells and the expression of pro-inflammatory cytokines were significantly attenuated by the administration of Pls [13]. However, the precise mechanism of the Pls-induced suppression of inflammatory responses remained mostly elusive.

Toll-like receptors (TLRs), a family of receptor proteins, play a wide role in innate and adaptive immune responses upon the stimulations by exogenous and endogenous TLRs ligands. Among TLRs, the TLR4 in particular has attracted a major attention due to its ability to recruit different adaptor proteins. The LPS-TLR4 complex initiates the TLR4 endocytosis, which

**Electronic supplementary material** The online version of this article (https://doi.org/10.1007/s12035-018-1307-2) contains supplementary material, which is available to authorized users.

✉ Md. Shamim Hossain
shamim@physiol.med.kyushu-u.ac.jp

[1] Department of Integrative Physiology, Graduate School of Medical Sciences, Kyushu University, Fukuoka 812-8582, Japan

[2] Department of Neuroinflammation and Brain Fatigue Science, Graduate School of Medical Sciences, Kyushu University, Fukuoka 812-8582, Japan

[3] Department of Medicine and Biosystemic Science, Kyushu University Faculty of Medicine, Graduate School of Medical Sciences, Kyushu University, Fukuoka 812-8582, Japan

is believed to play a major role in regulating inflammatory signals to induce the cytokine expression [14] by activating the Toll/interleukin-1 receptor (IL-1R) domain-containing adaptor protein (TIRAP) and MyD88 adaptor proteins, as well as Toll/IL-1R domain-containing adaptor inducing type I interferons (TRIF)-mediated pathways in mouse macrophages and Ba/F3 cells [15, 16]. The internalization of TLR4 has been reported to be mediated by clathrin-dependent endocytosis in human embryonic kidney (HEK 293) cells [17], lipid raft-mediated endocytosis in Chinese hamster ovary (CHO) cell line [18] and both clathrin-dependent and lipid raft-mediated endocytosis in cortical astrocytes [19]. However, there is a controversy about the role of lipid rafts in TLR4 signaling. The TLR4 is activated upon binding to the ligand, LPS, and undergo homodimerization and recruitment into the lipid rafts, thereby inducing the activation of nuclear factor (NF)-κB and pro-inflammatory gene expression in a murine pro-B cell line [16]. In contrast, it is also shown that lipid raft-dependent endocytosis of TLR4 suppresses signaling by accelerating degradation of TLR4 in macrophages [20].

Caspases are cysteine aspartate-specific proteases and have been recognized as crucial initiators of apoptosis and neurodegeneration [21]. These family proteins are associated with inflammation [22]. Among different caspases, caspase-3 is of particular interest because it is found to be associated with the pathologies of neurodegenerative diseases, such as AD [23, 24]. Recent studies also reported that caspase-3 is associated with the formation of amyloid-β by processing of amyloid precursor protein [25]. Caspase-8 and caspase-3 have been implicated in microglial activation by regulating protein kinase C [26]. Based on our previous findings that Pls inhibited the LPS-induced amyloid-β formation and microglial activation in the mouse cortex [13], we hypothesized that Pls can modulate caspase-8 and caspase-3 signaling in microglial cells, particularly, in the downstream of TLR4 activation to inhibit neuroinflammation.

In our present study, we explored the inflammatory pathway in BV2 and primary cultured microglial cells treated with LPS and found that the LPS-induced inflammatory signaling was associated with endocytosis of TLR4. In in vitro culture, the pretreatment with sPls (scallop-derived Pls) attenuated the LPS-induced signaling by inhibiting the dynamin-dependent internalization of TLR4. Knockdown of the Pls synthesizing enzyme, glyceronephosphate O-acyltransferase (GNPAT), by lentiviral vectors encoding short hairpin (sh)-RNA against GNPAT resulted in the increased activation of caspases and the endocytosis of TLR4. We previously found that Pls are reduced in the brain of aged mice and the AD model mice [27]. Interestingly, we found a significant increase in the endocytosis of TLR4 in these mice brains and the sPls drinking significantly reduced the TLR4 endocytosis in the AD model mice brain, suggesting that the Pls contents in the brain is closely associated with the TLR4 signaling and microglial activation.

## Methods

### Cell Line and Reagents

Human embryonic kidney derived cell lines, HEK293 and HEK293FT, were purchased from the Health Science Research Resources Bank, RIKEN, Japan. The BV2 immortalized cell line was a gift from Dr. Hidetoshi Saitoh, Kyushu University, Japan. Cells were maintained in Dulbecco's modified Eagle medium (DMEM) (Nissui Pharmaceutical, Tokyo, Japan) containing 10% heat-inactivated fetal bovine serum (FBS) (Invitrogen, Carlsbad, CA, USA), 50 μg/ml penicillin and 50 μg/ml streptomycin (Invitrogen), and glucose (1000 mg/L) at 5% $CO_2$ incubator set with the temperature of 37 °C. Highly pure Pls were extracted from scallop as reported previously [28, 29]. Since ethanolamine Pls (Pls-Etn) are enriched mostly in the brain [30], we further purified Pls-Etn from scallop Pls. The composition of fatty acids of Pls-Etn was analyzed using high-performance liquid chromatography method as previously described [29] and shown in Table 1. sPls were dissolved in water to the stock concentration of 5 mg/ml immediately before use. We used the following reagents; LPS (Sigma-Aldrich, St. Louis, MO, USA), cleaved caspase-3 inhibitor Z-DEVD-fmk (SC-311558; Santa Cruz Biotechnology, Dallas, TX, USA), caspase family inhibitor Z-VAD-fmk (SC-3067; Santa Cruz), dynamin inhibitor, dynasore (Sigma-Aldrich), and lipid raft inhibitor, methyl-β-cyclodextrin (MβCD, Sigma-Aldrich).

### Mice Experiments

All the experiments of mice were approved by the animal ethics committee of Kyushu University. The triple transgenic mice expressing the mutant APP, PS1, and Tau [31] were used as AD model mice. The AD model mice were treated with sPls containing water for 15 month and sacrificed at their age

**Table 1** The fatty acid composition of the ethanolamine Pls in the purified Pls

| Numerical symbol | | Percent |
|---|---|---|
| 16:0 | Palmitic acid | 5.2 |
| 18:0 | Stearic acid | 2.0 |
| 18:1, *n*-9 | Oleic acid | 2.6 |
| 18:2, *n*-6 | Linoleic acid | 1.2 |
| 18:3, *n*-3 | α-Linolenic acid | 1.0 |
| 20:4, *n*-6 | Arachidonic acid | 9.0 |
| 20:5, *n*-3 | Eicosapentaenoic acid (EPA) | 23.9 |
| 20:6, *n*-3 | Docosahexaenoic acid (DHA) | 38.9 |
| Others | | 16.2 |
| Total | | 100.0 |

of 18 month to see the endocytosis of TLR4. Young and old B6 mice (C57BL/6J) were purchased from the Kyudo Co Ltd., Japan. All efforts were made to minimize the number and suffering of mice throughout this study.

## Primary Microglial Cell Culture

Primary microglia cells were isolated from the cerebral cortex of 3-day-old mice according to our previously published report [32]. In brief, whole brains of neonatal mice were taken under sterile condition. The skin, blood vessels, and meninges were carefully removed, and the cerebral cortex was collected in a conical tube containing phosphate-buffered saline (PBS)-glucose (1 M glucose). The solution was then replaced by a PBS-bovine serum albumin (BSA) glucose solution followed by subjected to digestion with trypsin in 37 °C incubator for 10 min. We then neutralized the trypsin activity by adding FBS and added warmed DMEM medium followed by pipetting for 20 times to dissolve the tissue. The cell suspension was then filtered using 70-μm nylon cell strainers and then transferred to the 75 $cm^2$ 250 ml flask with DMEM medium supplemented with 10% FBS. The flasks were then incubated in a 5% $CO_2$ incubator at 37 °C for 2 weeks with the replacement of fresh medium every 5 days. After obtaining a confluent cell layer on the dish, the neonatal primary microglia cells were harvested by vigorous shaking of the flask. The microglial suspension was then centrifuged at 1000 rpm for 5 min followed by suspending the microglia pellets in FBS containing DMEM medium. The cell suspension was plated on the coverslip placed in the 12 well dishes with the density of $2 \times 10^3$ cells/well.

## Real-time Polymerase Chain Reaction (PCR)

Total RNA was extracted by TRIZOL reagent (Life Technologies) according to the recommended protocol. The cDNA was synthesized from the purified RNA using the Rever Tra Ace qPCR reverse transcriptase kit (Toyobo Co., Osaka, Japan). Real-time PCR was done by using SYBER premix Ex. Taq (TAKARA Bio Co., Shiga, Japan) in ABI 7500 real-time PCR system (Applied Biosystems, Foster City, CA). The data was analyzed by delta Ct technique considering the housekeeping gene, glyceraldehyde-3-phosphae dehydrogenase (GAPDH), as an internal control. The sequences of primer pair used in real time PCR were as following: *GAPDH*, forward 5'-CAATGTGTCCGTCGTGGATCT-3′ and reverse 5'GTCCTCAGTGTAGCCCAAGAT-3′; *TNF-α*, forward 5'-AAGCCTGTAGCCCACGTCGT-3′ and reverse 5'-AGGTACAACCCATCGGCTGG-3′; *IL-1β*, forward 5'-AAAAAAGCCTCGTGCTGTCG-3′ and reverse 5'-GTCG TTCTTGGTTCTCCTTG-3′.

## Western Blot Analysis

To extract proteins, microglia cell lines were suspended in radio-immunoprecipitation assay (RIPA) lysis buffer (1% NP-40, 0.5% sodium deoxycholate and 0.1% SDS dissolved in × 1 Tris-buffered saline (TBS) buffer) supplemented with a protease-phosphatase inhibitor cocktail (Roche). After 30 min on ice, cells were sonicated on the ice-cold water followed by centrifugation at 14000 rpm for 10 min to get rid of insoluble cell debris. Protein concentration was measured by the bicinchoninic acid (BCA) protein assay kit (Thermo scientific), and a total of 50 μg protein was loaded onto 6–15% sodium dodecyl sulfate–polyacrylamide gel electrophoresis (SDS-PAGE) and blotted onto nitrocellulose membranes (BIO-RAD). The membranes were then blocked with TBS buffer supplemented with 5% Difco skim milk. Membranes were incubated overnight at 4 °C with the following antibodies: rabbit anti-cleaved caspase-3, rabbit anti-cleaved caspase-8 and rabbit anti-cleaved polyadenosine diphosphate ribosepolymerase1 (PARP1) (1:1000; cell signaling technology), rabbit anti-GNPAT (1:1000; Abcam), mouse anti-p65 (Cell signaling), rabbit anti-Lamin B (Cell signaling), and goat anti-mouse antibody β-actin (1:1000; Santa Cruz). After washing, membranes were incubated with the appropriate horseradish peroxidase-coupled goat anti-rabbit or anti-mouse IgG secondary antibody (cell signaling technology) at room temperature for 2 hours. Proteins were visualized with Super Signal West Pico Chemiluminescent Substrate (Thermo scientific) using the ImageQuant LAS4010 machine (GE Healthcare). Quantification of the images performed by the ImageJ software [12]. The nuclear fraction assays using the cells were performed according to our previous publication [27].

## Preparation of sh-RNA Lentiviruses and Cell Transfection

The cloning of sh-RNAs was performed by the previously published protocol [27]. Simply, the sh-RNA sequence was cloned into the pLL3.7 lentiviral vector following the protocol provided in the Addgene website (Plasmid 11,795). The target sequences were as follows: sh-Luc: (5′-CTTA CGCTGAGTACTTCGAG-3′) and sh-GNPAT: (5′-GTCC CAATTAGCATCAGT-3′). For the viral production, HEK-293 FT cells were transfected with the cloned pLL3.7 vectors along with the vectors pMD2.G (Addgene plasmid 12,259), pRSV-Rev (Addgene plasmid 12,253), and pMDLg/pRRE (Addgene plasmid 12,251). After 72 hours from transfection, HEK-293FT cells supernatant were collected and used for infection of the target BV2 cells with the lentivirus particles, $5 \times 10^5$ TDU (transduction unites), in a 6-cm dish culture for 48 h.

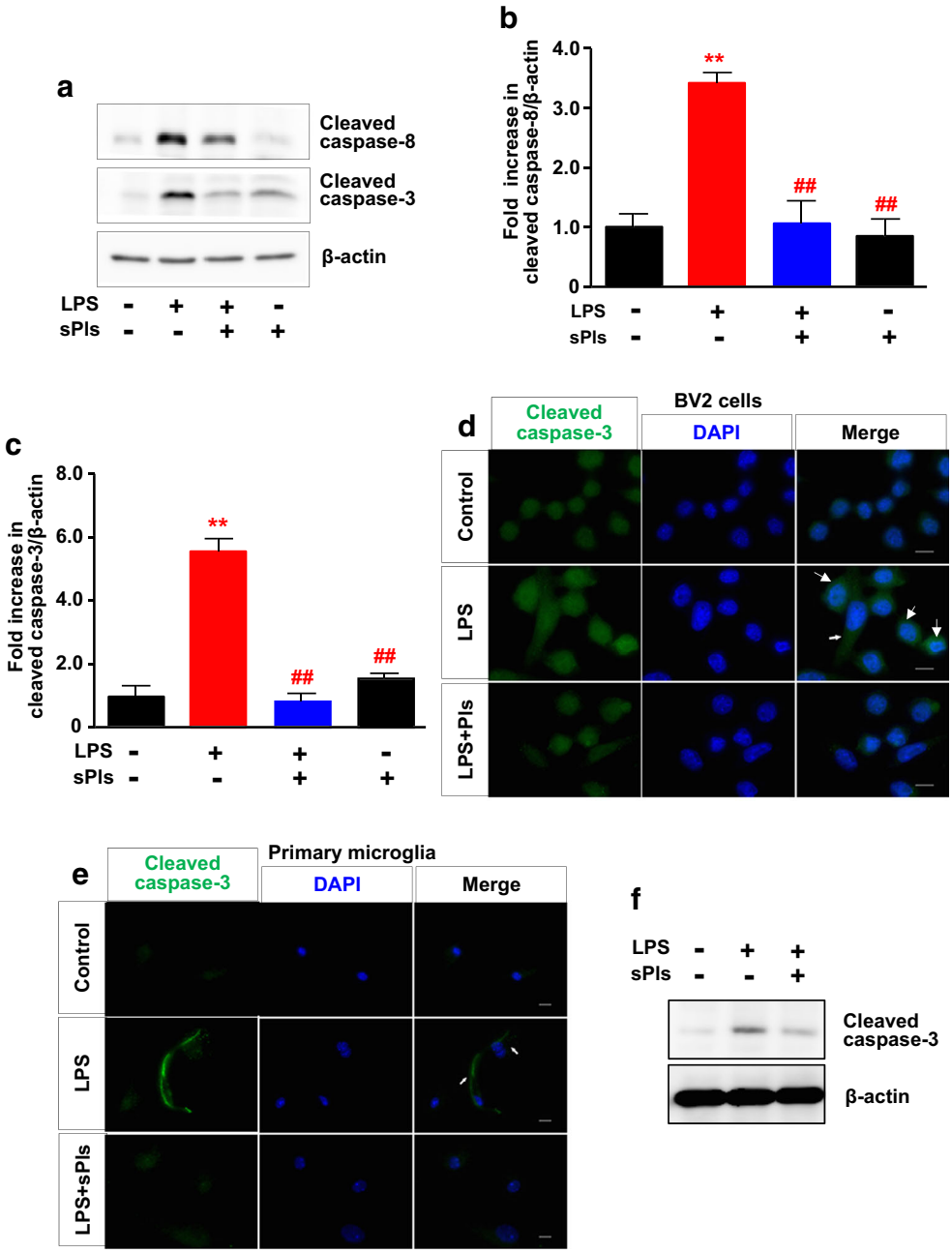


**Fig. 1** Pls inhibit cleavage of caspase-8 and caspase-3 upon LPS stimulation. **a**–**c** Western blotting data showed that LPS (1 μg/ml) treatments for 6 h induced cleavage of caspase-8 (**a** and **b**) and caspase-3 (**a** and **c**) in BV2 microglial cells, which were completely blocked by the pretreatments with 5 μg/ml of sPls for 12 h. Statistical analysis from the image intensities values showed that sPls significantly inhibited cleavage of caspase-8 (**$P < 0.01$ vs. control, $^{\#\#}P < 0.01$ vs. LPS, Bonferroni's test, $n = 3$) and caspase-3 (**$P < 0.01$ vs. control group, $^{\#\#}P < 0.01$ vs. LPS group, $n = 3$). Beta-actin was used as a loading control. **d, e** Under the same experimental condition of panel (**a**), the immunocytochemistry data in BV2 cells (**d**) and primary microglia (**e**) showed that the LPS treatment-induced increase in cleaved caspase-3 (green, white arrows) was attenuated by Pls pretreatment. Similar to the immunostaining data of primary microglial cells (**e**), we also noticed the reduction of cleaved caspase-3 in the western blotting assays (**f**). The data represents three independent experiments. Scale bars, 10 μm

## Immunocytochemical (ICC) and Immunohistochemical (IHC) Assays

The BV2 and primary microglia cells were plated in 12-well dishes containing 15-mm coverslips overnight. Some cells were treated with Pls (5 μg/ml) for 6 h followed by LPS (1 μg/ml) for 3 and 6 h. Other cells were treated by dynasore (40 μM) for half hour followed by LPS (1 μg/ml) treatments for 3 and 6 h. Some other groups were treated by Z-DEVD-fmk (20 μM) for 1 h followed by LPS (1 μg/ml) treatments for 3 and 6 h. Cells were then fixed with 4% paraformaldehyde in PBS for 30 min at 4 °C. The fixed cells were then permeabilized using the PBS containing 0.1% Triton X-100, and then the cells were blocked with 3% BSA in PBS. Cells were incubated with primary antibodies dissolved in 3% BSA-PBS rabbit anti-cleaved caspase 3 (1:300; cell signaling), mouse anti-P65 NF-κB (1:1000; cell signaling), rabbit anti-TLR4 (1:500; Santa Cruz biotechnology), and mouse anti-Rab-5 (1:500; Santa Cruz biotechnology) overnight at 4 °C. The rinsed cells were incubated with Alexa Fluor 488 green/568 red labeled secondary antibody (1:1000, Invitrogen) mixes for 2 h at room

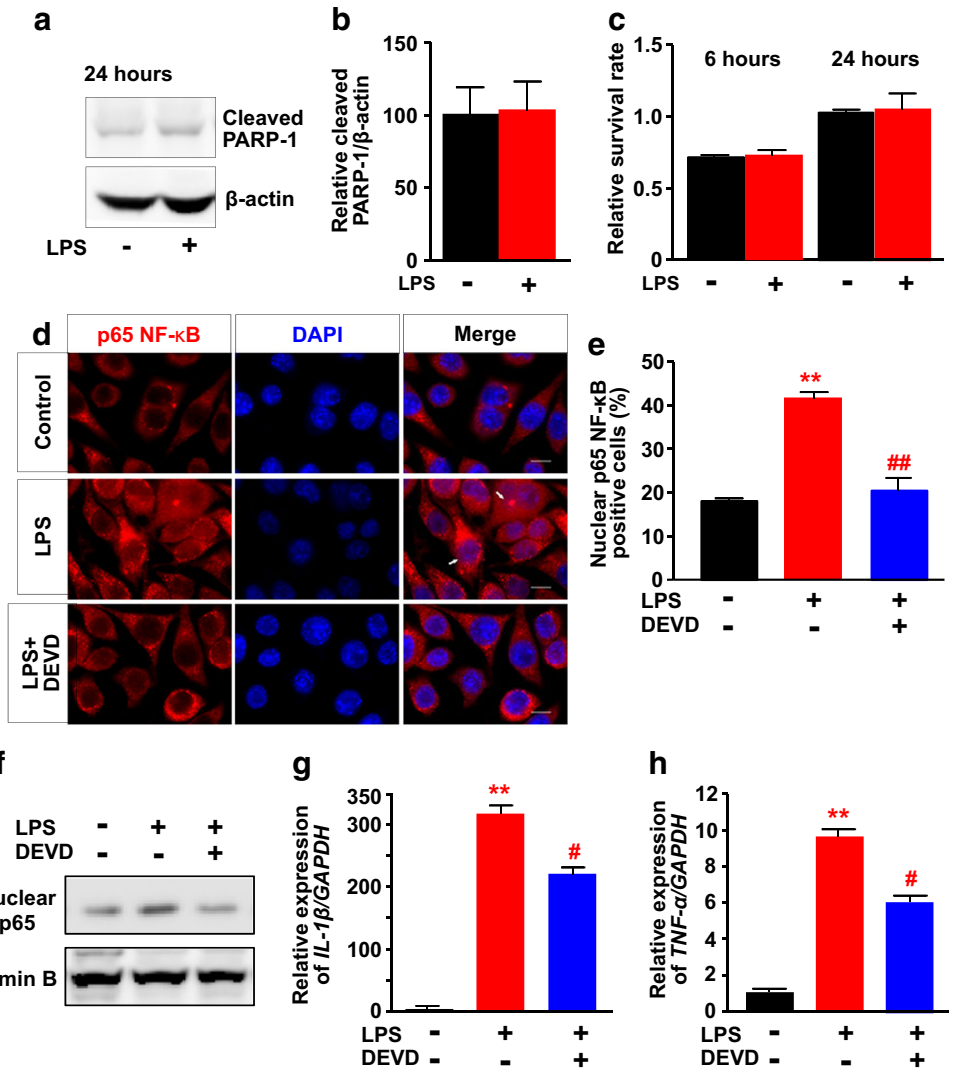


**Fig. 2** LPS-induced NF-κB activation and cytokine expression are attenuated by a caspase-3 inhibitor in BV2 cells. **a** Twenty-four hours after treatment with LPS (1 μg/ml), Western blotting assay showed an unchanged level of cleaved PARP-1. **b** The images of panel (a) were quantified and plotted as graphs. **c** Cell survival assay showed that there was no cell death at 6 and 24 h after LPS (1 μg/ml) application. **d** BV2 cells were pretreated with 20 μM/ml Z-DEVD-fmk (DEVD, a caspase-3 inhibitor) for 1 h before the LPS (1 μg/ml) treatment. ICC studies using p65 antibody (red) and DAPI (nuclear staining, blue) were performed 6 h after LPS treatment. The LPS-induced nuclear translocation (white arrows in the middle row) was attenuated by DEVD (bottom). Scale bars, 10 μm. **e** NF-κB nuclear translocation was assessed and quantified as the percentage of the p65 nuclei positively stained cells to the total cells (**$P < 0.01$ vs. control group, $^{\#\#}P < 0.01$ vs. LPS group, $n = 3$). **f** The Western blotting data of the nuclear p65 expression and the nuclear marker lamin B in the same experimental condition of panel (**d**–**e**). The data represents three independent experiments. **g**, **h** Real-time PCR analysis showed that the relative expression of *IL-1β* (**g**) and *TNF-α* (**h**) were significantly attenuated by the DEVD pretreatments in BV2 cells (**$P < 0.01$ vs. control group, $^{\#}P < 0.05$ vs. LPS group, $n = 5$)

temperature. Every treatment was followed by washing 3 times for 5 min with cold PBS. Coverslips were mounted with 4′,6-diamidino-2-phenylindole (DAPI) containing Fluoromount-G (southern Biotech) medium to detect cell nuclei. Immunofluorescence images were collected by the lifetime imaging microscope (Keyence, BZ-9000 series and BZ-X700 series). The IHC studies were carried out by the previously published protocol [27]. We have quantified the co-localization of Rab-5 and TLR4 using the image analyzer software (BZ-X analyzer) that comes with the Keyence microscope (BZ-X700).

## Cell Proliferation (WST8) and Liquid Chromatography-Electronspray Ionization-Tandem Mass Spectrometry (LC-MS) Assays

Cells were treated with sPls (5 μg/ml) for 12 h, followed by LPS (1 μg/ml) for 6 and 24 h. The viable cells were

measured by cell counting kit-8 (Dojindo Molecular Technologies). The absorbance was measured at 450 nm using the microplate reader (BioRad) and data was represented relatively to control groups [12]. To quantify the total ethanolamine Pls in the cells, the cell extracts were subjected to the lipid analysis as described before [27]. A total of 50 μg protein extracts from each group of cells were analyzed.

## Statistics

Results were expressed as the mean ± SEM (standard error of mean). The real-time PCR data, western blot pixel quantification, and WST-8 assay data were analyzed using one-way analysis of variance (ANOVA) followed by the Bonferroni's test for a comparison of paired groups. Moreover, t-Test was used to analyze the significance of two group experiments. All statistical tests were carried out using Graph Pad Prism. The data were expressed as mean ± SEM and values of $P < 0.05$ were considered to be statistically significant.

## Results

### Plasmalogens Attenuate Microglial Activation upon Inflammatory Stimulus

It has been demonstrated that the co-administration of Pls with LPS significantly attenuated the activation of microglia in mice [13], but the molecular mechanism behind the anti-inflammatory role of Pls remained elusive. It is to be noted that the Pls contents of the microglial cells were increased upon the extracellular treatments with purified sPls (data not shown). Since caspase signaling was recently implicated in microglial activation [26], we investigated the effect of sPls on caspase-8 activation and its downstream signaling in BV2 cells. As shown in Fig. 1a, b, the BV2 cells demonstrated an increase in cleaved caspase-8 protein after 6 h of 1 μg/ml LPS treatment compared with untreated cells, which was completely suppressed by the pretreatment with sPls at the dose of 5 μg/ml. Two more independent experiments showed similar results in microglial cells (Fig. S1). A significant increase in cleaved caspase-3, a downstream of caspase-8 pathway, after LPS treatment was also blocked by sPls pretreatment (Fig. 1c). ICC study showed that an increase in cleaved

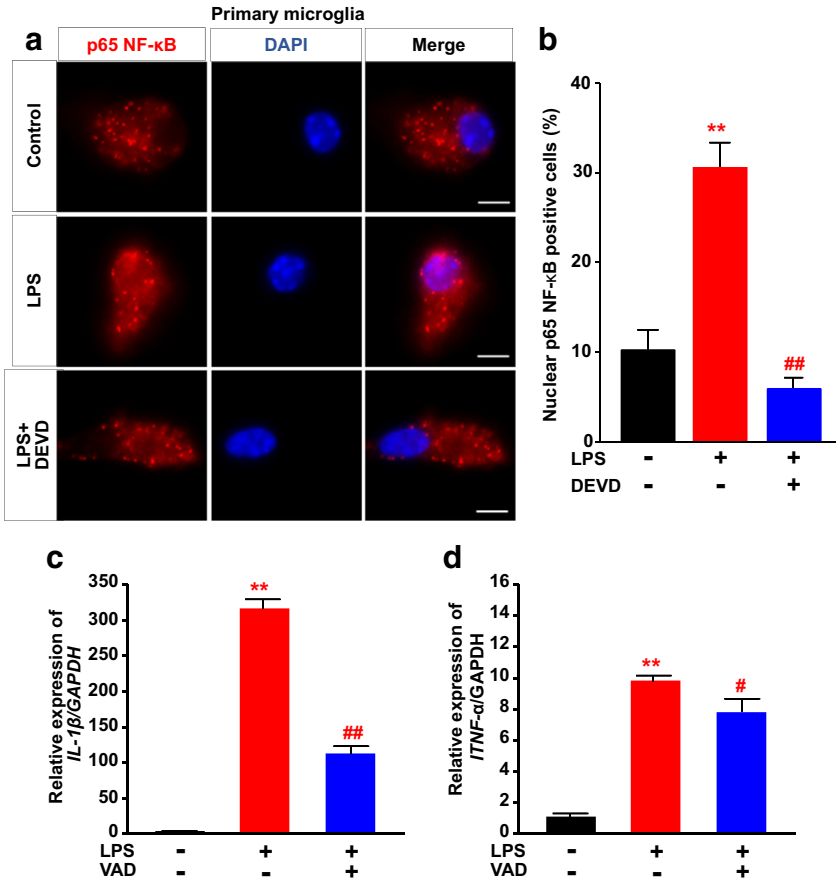


**Fig. 3** LPS-induced NF-κB activation and cytokine expression are attenuated by a caspase-3 inhibitor in primary microglial cells. **a** Primary microglial cells were pretreated with 20 μM/ml Z-DEVD-fmk for 1 h before the LPS (1 μg/ml) treatment. ICC studies using p65 antibody (red) and DAPI (nuclear staining, blue) were performed 6 h after the LPS treatment. The LPS-induced nuclear translocation (middle raw) was attenuated by DEVD (bottom). Scale bars, 5 μm. **b** The image intensities data showed a significant reduction of LPS-induced nuclear p65 positive cells by the caspase-3 inhibitor (**$P <$ 0.01 vs. control $^{\#\#}P < 0.001$ vs. LPS, $n = 3$). **c**, **d** Real-time PCR analysis showed that the LPS-induced expressions of *IL-1β* (**c**) and *TNF-α* (**d**) were significantly attenuated by a pan caspase inhibitor Z-VAD-fmk (VAD) in primary microglial cells (**$P <$ 0.01 vs. control group, $^{\#\#}P < 0.01$ and $^{\#}P < 0.05$ vs. LPS group, $n = 3$)

caspase-3 (green) upon the LPS stimulation (Fig. 1d, white arrows in the middle row) was abolished by pretreatment with sPls (Fig. 1d). Not only BV2 cell line but also the primary microglial cells showed an attenuation of the LPS-induced increase in cleaved caspase-3 by pretreatment with sPls (Fig. 1e). Similar to the ICC data, western blotting assays also show the inhibition of cleaved caspase-3 expression in the primary microglial cells by the Pls treatments (Fig. 1f).

## Inhibition of Caspase-3 Attenuates LPS-Induced Activation of NF-κB and Cytokines Expression

Although activation of caspases was known to play a role in the initiation and regulation of cell apoptosis [33], we also focused the pro-inflammatory signaling induced by the activation of caspases in the microglia. The cells were treated with 1 μg/ml of LPS for 24 h and analyzed for the apoptotic marker, cleaved PARP1. In our experimental condition, we did not notice any increases in the cleaved PARP protein 24 h after the LPS treatment (Fig. 2a, b). Furthermore, the cell viability analysis showed that the LPS treatments for 6 and 24 h did not change the microglial cell survival rate (Fig. 2c). These findings shown in Fig. 1 and Fig. 2a–c suggest that the LPS treatments activate caspases in this limited time points without inducing a cell death. To investigate if the caspase-3 activation could initiate the pro-inflammatory responses in microglial cells, we have employed the caspase-3 inhibitor (Z-DEVD-fmk, DEVD) to see the changes in the nuclear translocation of cytoplasmic p65, which is well considered as a key step in the activation of the NF-κB signaling [34]. As shown in Fig. 2d, e, the nuclear localization of p65 NF-κB in BV2 cells was significantly increased after the LPS treatments, which was completely abolished by the pretreatment with the DEVD inhibitor. In consistent with the immunofluorescence data, western blotting assay showed similar evidences that DEVD treatments effectively inhibited the nuclear localization of p65 protein (Fig. 2f). Furthermore, the LPS-mediated increases in the gene expression of pro-inflammatory cytokines, *IL-1β* and *TNF-α*, were also inhibited by the pretreatments of DEVD in BV2 microglial cells (Fig. 2g, h). The inhibitory

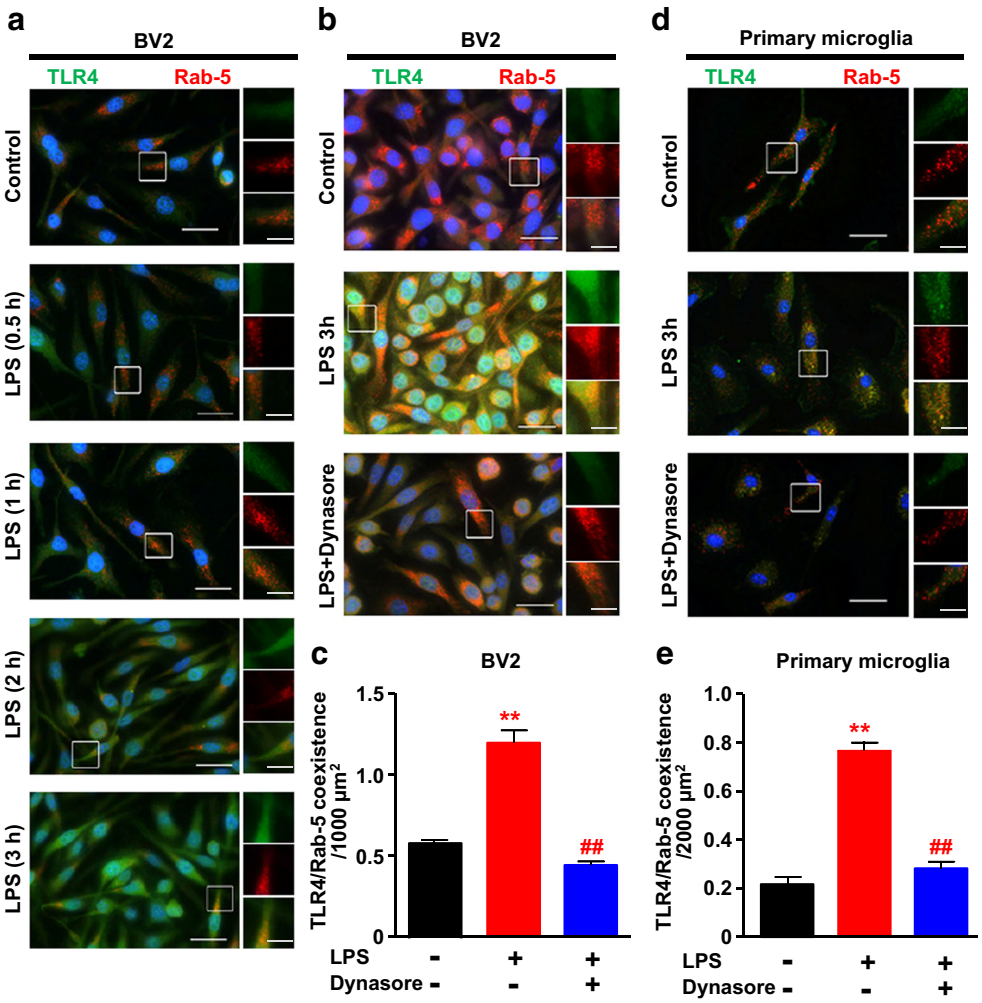


**Fig. 4** LPS treatment induces endocytosis of TLR4 in a dynamin-dependent manner. **a** BV2 cells were stimulated with 1 μg/ml of LPS for 0.5, 1, 2, and 3 h followed by ICC studies with TLR4 (green) and the early endosomal marker Rab-5 (red) antibodies. Scale bars, 25 μm. Small panels on the right side of each big panel show the white square area at a higher magnification stained with TLR4 (upper), Rab-5 (middle), and merged (bottom). Scale bars, 10 μm. **b**-**e** Coexistence of TLR4 and Rab-5 observed 3 h after LPS (1 μg/ml) treatment was abolished by pretreatment with dynasore (40 μM, 30 min) in BV2 cells (**b**) and primary microglial cells (**d**). The image quantification data show the significant reduction of the coexistence by the dynasore pretreatments in BV2 cells (**c**) and primary microglial cells (**e**). (**$P < 0.01$ vs. control group, and ##$P < 0.01$ vs. LPS group, $n = 3$)

effect of DEVD on the LPS-induced nuclear localization of p65 was also observed in the primary microglia (Fig. 3a, b). In addition, the LPS-induced pro-inflammatory cytokine expression was attenuated by a pan caspase inhibitor Z-VAD-fmk (VAD) (Fig. 3c, d), suggesting that the caspase activation is a key event to induce the pro-inflammatory gene expression upon the LPS treatment in the microglial cells.

## LPS Treatment Induces Endocytosis of TLR4 in Microglia

Endocytosis of TLR4 is shown to be a critical step for the induction of inflammatory signals in cortical astrocytes [19]. To our knowledge, this endocytosis process had not been studied so far in microglial cells. To evaluate the possibility that the LPS treatments could promote TLR4 endocytosis in the microglia, the coexistence of TLR4 with the early endosome marker protein, Rab-5, in BV2 cells was investigated at different time points after the LPS treatments. As shown in Fig. 4a, the TLR4 (green) merged with Rab-5 (red) becoming yellow at 2 h after LPS (1 μg/ml) treatment and reached a steady-state level by 3 h, indicating the endocytosis of TLR4 into the endosome. It has been shown that dynamin played a critical role in the endocytosis of TLR4 in macrophages [15]. We, therefore, examined the effect of a dynamin inhibitor (dynasore) on TLR4 internalization in microglial cells. The results showed that the pretreatment with 40 μM dynasore for 30 min completely blocked the LPS-mediated TLR4 endocytosis in BV2 cells (Fig. 4b, c). Furthermore, the coexistence of TLR4 with Rab-5 following LPS treatment was also blocked by pretreatment with dynasore in primary microglia (Fig. 4d, e).

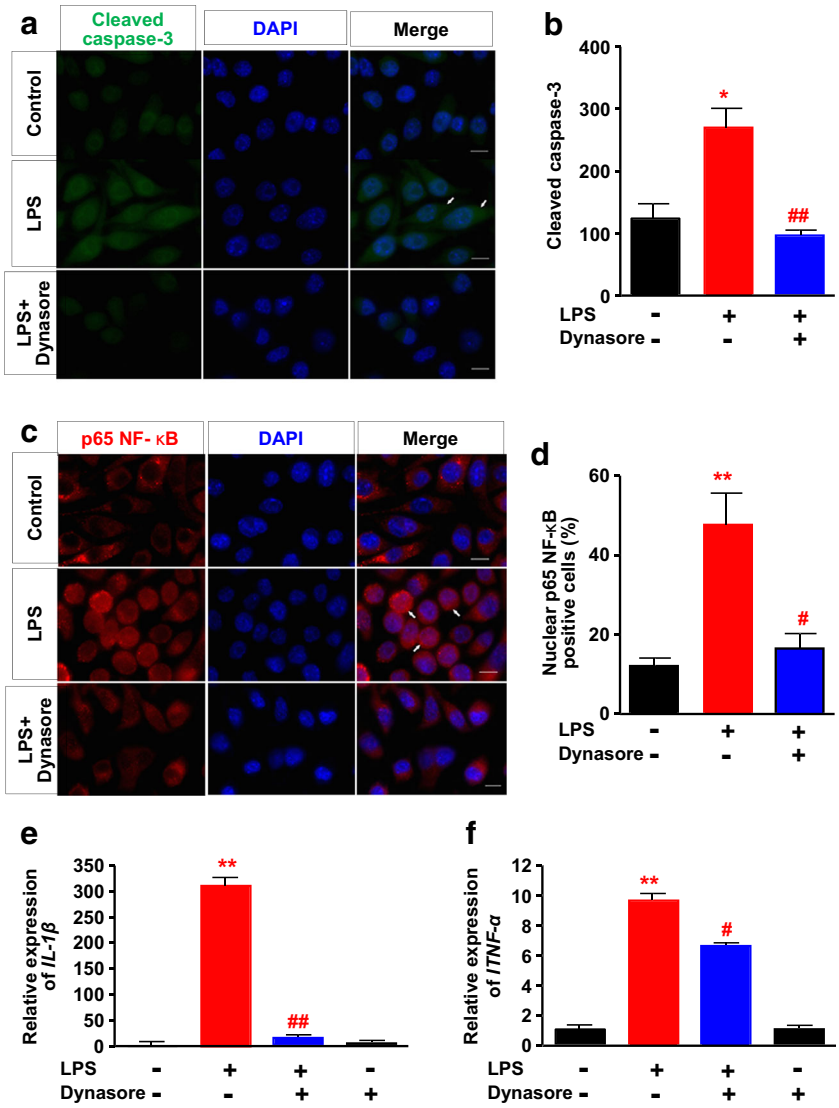


**Fig. 5** The dynamin inhibitor cancels the LPS-induced activation of caspase-3 and nuclear localization of p65 in BV2 cells. **a** BV2 cells were pretreated with 40 μM/ml dynasore (a dynamin inhibitor) for 30 min followed by LPS (1 μg/ml) for 6 h. ICC studies showed that the LPS-induced enhancement of cleaved caspase-3 immunoreactivity (green, white arrows in the middle row) was completely suppressed by dynasore. **b** Image quantification data showed a significant suppression of the LPS-mediated increase in caspase-3 by the dynasore pretreatment ($^{*}P < 0.05$ vs. control, $^{\#\#}P < 0.01$ vs. LPS group, $n = 3$). **c** The LPS-induced nuclear localization of p65 (red or violet, white arrows in the middle row) was also inhibited by dynasore. DAPI staining indicates nucleus. **d** Image quantification data showed the significant inhibition of the LPS-mediated increase in nuclear localization of p65 ($^{**}P < 0.01$ vs. control group, $^{\#}P < 0.05$ vs. LPS group, $n = 3$). **e**, **f** Real-time PCR assays demonstrated that the dynasore pretreatments canceled the LPS-mediated induction of *IL-1β* (**e**) and *TNF-α* (**f**) ($^{**}P < 0.001$ vs. control group, $^{\#\#}P < 0.01$ and $^{\#}P < 0.05$ vs. LPS group, $n = 3$)

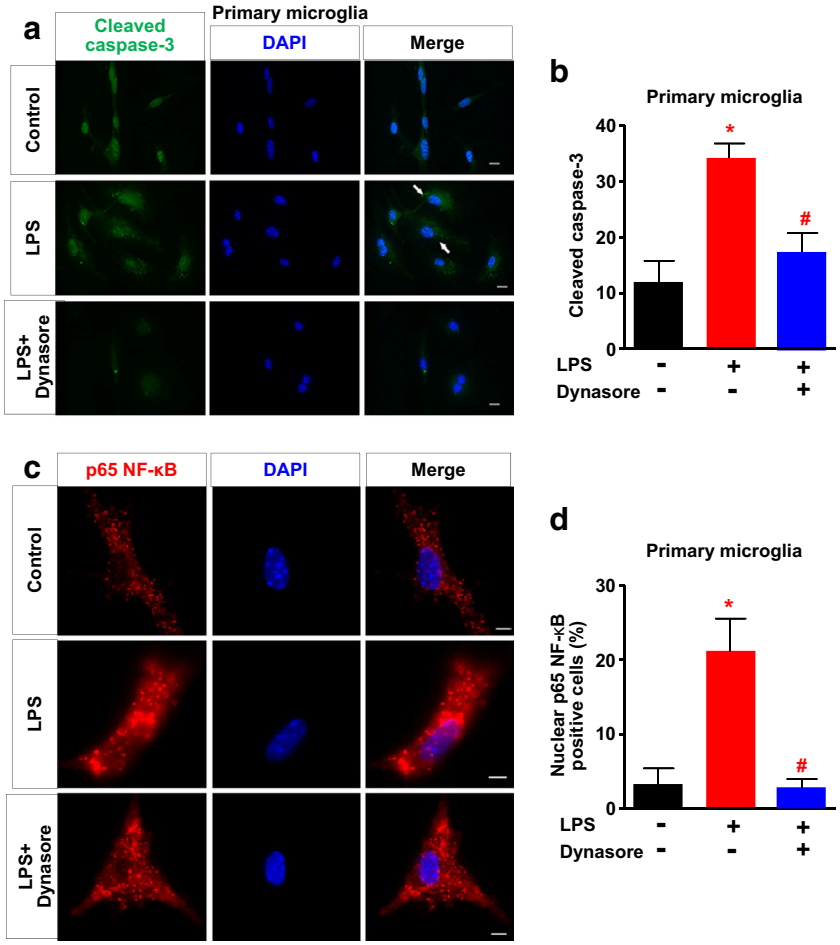


**Fig. 6** Dynamin inhibitor cancels the LPS-induced caspase-3 activation and nuclear localization of p65 in primary microglial cells. **a**, **b** Primary microglial cells were pretreated with 40 μM/ml dynasore (a dynamin inhibitor) for 30 min followed by LPS (1 μg/ml) treatments for 6 h. ICC studies (**a**) and the quantification of the data (**b**) showed the LPS-mediated increase in cleaved caspase-3 (green, white arrows in the middle row) was significantly reduced by the dynasore pretreatments. **c**, **d** Under the same experimental condition of panel (**a**), primary microglial cells were stained with p65 antibody (**c**). The LPS-mediated increase in nuclear p65 was significantly reduced by the dynasore pretreatment (**d**) ($^{*}P < 0.05$ vs. control; $^{\#}P < 0.05$ vs. LPS, $n = 3$). Scale bars, 5 μm

## LPS-induced Caspase-3 Activation Requires Dynamin-Mediated Endocytosis of TLR4

We examined whether the endocytosis of TLR4 was important for the LPS-induced inflammatory responses such as the activation of caspases and nuclear translocation of NF-κB. As shown in Fig. 5a, b, the pretreatment with dynasore effectively prevented the sustained LPS-induced caspase-3 activation in BV2 cells. ICC study showed that the nuclear localization of p65, downstream signal of the caspase-3 activation, was not increased by the LPS in the cells pretreated with dynasore (Fig. 5c, d). Furthermore, the LPS-induced increases in expression of *IL-1β* and *TNF-α* were significantly blocked by the dynasore pretreatments (Fig. 5e, f), suggesting that the internalization of TLR4 is important for the NF-κB activation followed by the cytokines expression. The pretreatment with dynasore also inhibited the LPS-induced caspase-3 activation (Fig. 6a, b) and p65 nuclear localization (Fig. 6c, d) in primary microglia. Interestingly, the LPS-induced endocytosis of TLR4, which was demonstrated by the yellow color merged with TLR4 (green) and Rab-5 (red) as shown in Fig. 7a, middle panel, was maintained after the pretreatment with a caspase-3 inhibitor (Z-DEVD-fmk, DEVD) (bottom panel) in BV2 cells. The same results were obtained from primary glial cells (Fig. 7c, d). The failure of blocking the LPS-induced endocytosis of TLR4 by the caspase inhibitor suggested that the TLR4 endocytosis was the upstream event of the caspase activation during the LPS-induced neuroinflammation process. Our findings for the first time suggest that the dynamin-mediated microglial endocytosis of TLR4 occurs first to activate caspase-3, thereby leading to the nuclear localization of NF-κB to induce pro-inflammatory responses.

## sPls Attenuate Caspase-3 by Inhibiting LPS-induced Endocytosis of TLR4 in Microglial Cells

After elucidating the molecular mechanisms of the LPS-induced pro-inflammatory responses in microglia, we sought to investigate how sPls attenuated the activation of caspases by LPS (Fig. 1). In an attempt to characterize the molecular events of Pls that hinder the active caspase-3 in the process of microglial activation, we tested if sPls might inhibit the endocytosis of TLR4, which was a prerequisite step of the LPS-induced inflammation. As shown in Fig. 8a, b, ICC studies

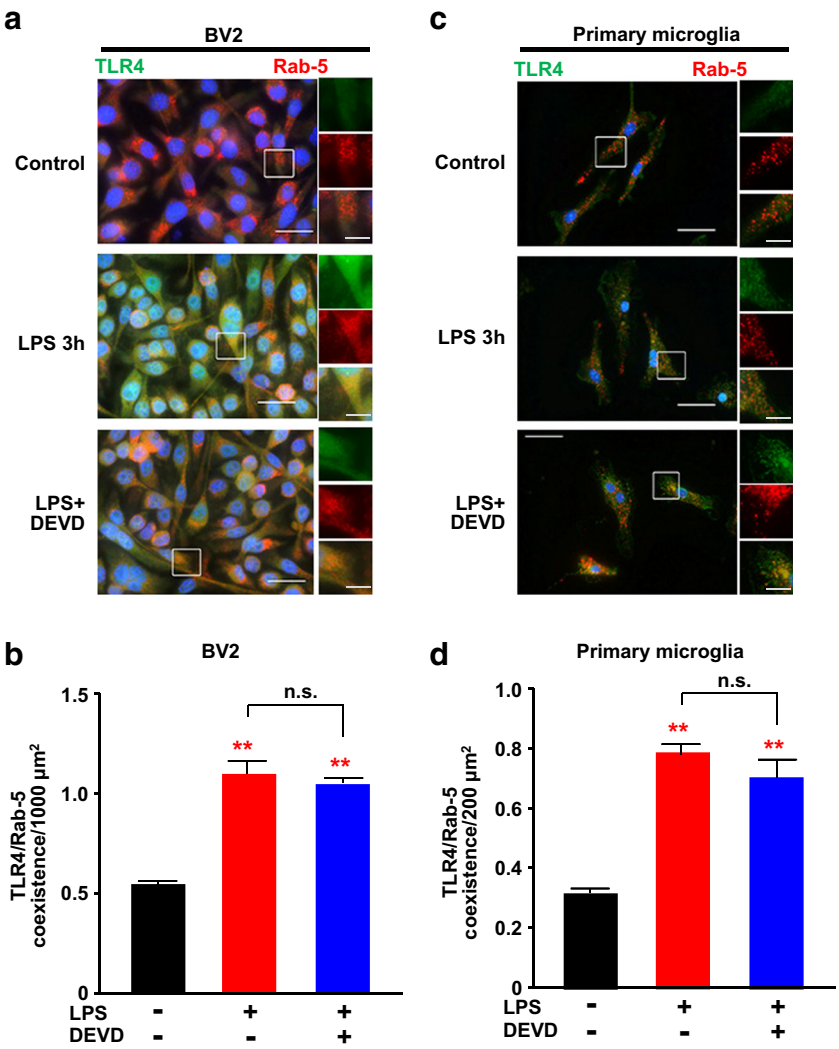


**Fig. 7** Caspase-3 inhibitor cannot cancel the LPS-induced internalization of TLR4 in microglial cells. **a**-**d** The cells were pretreated with a caspase-3 inhibitor, z-DEVD-fmk, (20 μM) for 60 min prior to 3 h LPS (1 μg/ml) treatments. ICC studies show the coexistence of TLR4 (green) with the Rab-5 (red) in BV2 cells (**a**) and in the primary microglial cells (**c**). Scale bars, 25 μm. Small panels on the right side of each big panel show the white square area at a higher magnification stained with TLR4 (upper), Rab-5 (middle), and merged (bottom). Scale bars, 10 μm. The quantification data of the images showed that the caspase inhibitor failed to reduce LPS-induced coexistence of TLR4 with Rab5 in BV2 cells (**b**) and in microglial cells (**d**) (**$P < 0.01$ vs. control group; n.s. stands for no significant differences between the groups, $n = 3$)

demonstrated that the BV2 cells after 3 h LPS stimulation displayed an increase the TLR4 coexistence with Rab-5 (orange color in the middle panel of Fig. 8a) compared with the untreated cells but the pretreatment with 5 μg/ml sPls dramatically attenuated this coexistence. Furthermore, it was noticed that the pretreatment of sPls decreased the TLR4 immunoreactivity (green in the bottom panel of Fig. 8a). Similar results were also obtained in the primary microglial cells demonstrating that the Pls pretreatment can attenuate the coexistence of TLR4 with Rab-5 upon the LPS stimulation (Fig. 8c, d). These findings suggest that the anti-inflammatory effect of sPls against LPS insult is due to the reduction of dynamin-mediated endocytosis of TLR4.

## Reduction of GNPAT Accelerate the Endocytosis of TLR4 in Microglial Cells

The reduction of microglial Pls was carried out by the knockdown of GNPAT in BV2 cells. The lentiviral mediated delivery of sh-GNPAT particles was effective in the reduction of cellular Pls (Fig. 11e). When we knockdowned GNPAT, we found a significant increase of TLR4 and Rab5 co-localization in the cells (Fig. 9a, b), suggesting that the reduction of GNPAT itself can enhance the endocytosis of TLR4 in the microglial cells. In addition, the LPS treatments for 6 h showed a significant increase of TLR4 localization with the endocytosis marker Rab5 in the sh-GNPAT group compared to the control sh-Luc group (Fig. 9a, b), suggesting that a reduction of GNPAT accelerate the LPS-mediated TLR4 endocytosis.

## Inhibition of Lipid Raft Function Abolishes the Attenuating Effect of Pls on LPS-induced *IL-1β* Expression

Since Pls were shown to localize in the lipid raft microdomain in the membrane and is associated with the membrane function [35-37], we examined a role of lipid rafts

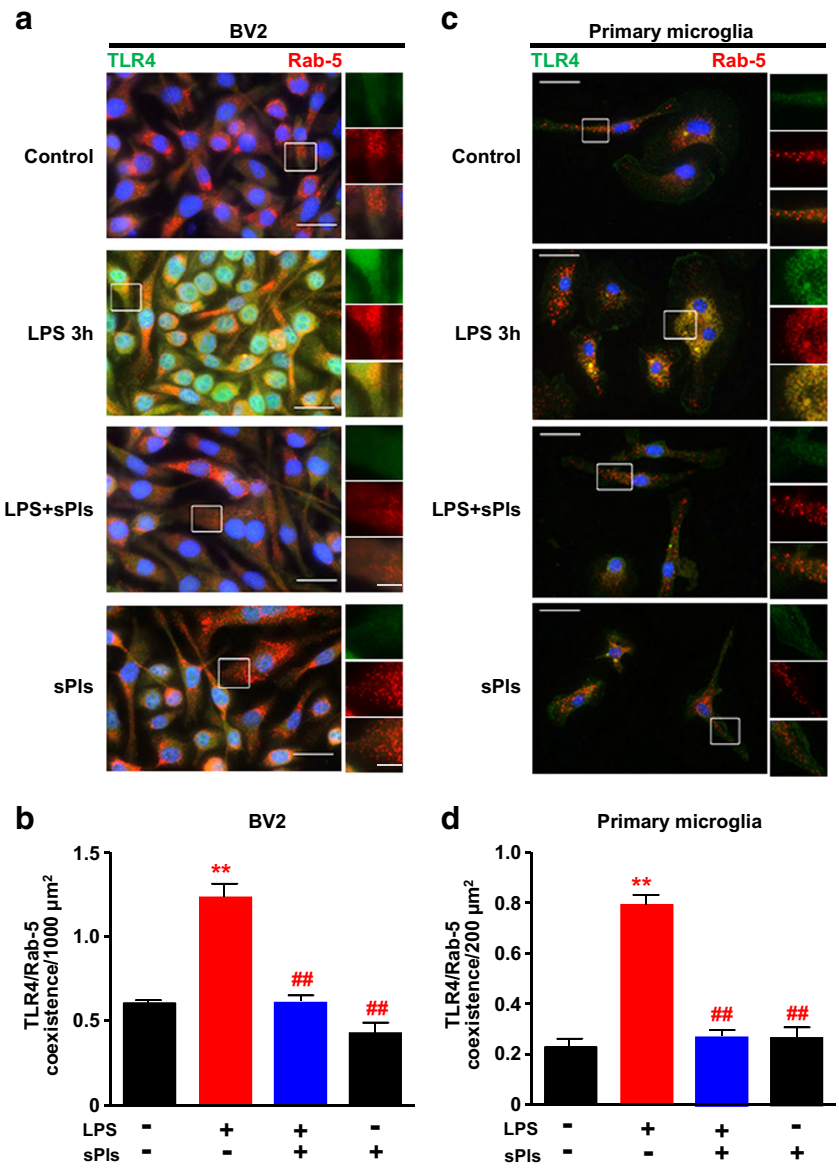


**Fig. 8** Pls attenuate LPS-induced endosomal internalization of TLR4 in microglia. **a**-**d** BV2 cells (**a**) and primary microglial cells (**c**) were pretreated with Pls (5 μg/ml) for 6 h prior to LPS (1 μg/ml) treatments for 3 h. The cells were then stained with TLR4 (green) and Rab-5 (red) antibodies. Scale bars, 25 μm. Small panels on the right side of each big panel show the white square area at a higher magnification stained with TLR4 (upper), Rab-5 (middle), and merged (bottom). Scale bars, 10 μm. Quantification data showed that the Pls pretreatments significantly reduced the LPS-mediated internalization of TLR4 in BV2 cells (**b**) and primary microglial cells (**d**) (**$P < 0.01$ vs. control group, $^{\#\#}P < 0.01$ vs. LPS group, $n = 3$)

in the Pls-induced attenuation of an inflammatory response. As shown in Fig. S2, the LPS-induced enhancement of IL-1β mRNA expression was attenuated by the pretreatment of sPls. However, the treatment with MβCD (5 μM), which was shown to deteriorate the lipid raft function by depleting membrane cholesterol [20, 37], completely blocked the effect of sPls. The MβCD treatment itself did not affect the LPS-induced enhancement of the *IL-1β* expression in our experimental condition.

## Knockdown of Pls Synthesizing Enzyme, GNPAT, by sh-RNA Activates Caspases in the Microglial Cells

Previous work from our group has shown that the reduction of Pls, mediated by the knockdown of a key enzyme for synthesizing Pls, GNPAT [38], increases the p65 NF-κB nuclear localization and the cytokine expression in the microglial cells [10]. We checked whether the knockdown of GNPAT is associated with the activation of caspase proteins. We used a lentivirus-based RNA delivery system to infect BV2 microglial cells with the sh-RNAs targeting GNPAT. The sh-GNPAT lentiviral particles markedly reduced the expression of GNPAT protein in BV2 cells (Fig. 10a, b). The GNPAT knockdown in the microglial cells was associated with the increased expression of cleaved caspase-8 (Fig. 10a, c) and caspase-3 (Fig. 10a, d) compared with the control sh-RNA (sh-Luc) infected cells, indicating that a reduction of GNPAT in the microglial cells could trigger the inflammatory responses. The GNPAT knockdown decreased the total ethanolamine Pls content in the cells (Fig. 10e). These findings suggest that cellular Pls can inhibit microglial inflammation possibly by attenuating the dynamin-mediated endocytosis of

TLR4, which is followed by the activation of caspases and nuclear localization of the p65 protein.

### TLR4 Endocytosis is Increased in the Brain of Aged and AD Model Mice

Previous work from our group has shown a reduction of Pls in the brains of aged mice and in the triple transgenic AD model mice [27]. In the present study, we analyzed the brain tissues by IHC studies and found a significant increase of TLR4 endocytosis compared with the control young mice brains (Fig. 11a, b). The endocytosis was measured by the merging of TLR4 signals with the endocytosis marker (Rab5) signals. To our knowledge, it is the first report that shows an increased co-localization of TLR4 with Rab5 in aged and AD model mice. These data suggest that the reduction of Pls in these brains is associated with the increased endocytosis of TLR4. Interestingly, sPls drinking reduced the endocytosis of TLR4 among the AD model mice (Fig. 11a, b).

## Discussion

In the present study, we found (1) that LPS treatments activated caspase-8 and caspase-3 in primary microglial cells and in BV2 cells, which did not induce cellular apoptosis, (2) that the LPS-induced nuclear localization of p65 NF-κB and expression of pro-inflammatory cytokines were mediated by the caspase activation, (3) that the LPS insult enhanced dynamin-dependent endosomal localization of TLR4 in microglial cells, (4) that the activation of caspases, nuclear localization of p65 NF-κB and expression of cytokines were all attenuated by the pretreatments with dynamin inhibitor (dynasore) indicating that the endocytosis of TLR4 played an important role in the LPS-induced signaling, (5) that pretreatment with a caspase-3 inhibitor (Z-DEVD-fmk) also inhibited the LPS-induced NF-κB activation and cytokine expression, but failed to inhibit the TLR4 internalization, suggesting that the endosomal recruitment of TLR4 was an earlier event of caspase activation, (6) that the pretreatments with sPls significantly attenuated the LPS-mediated endosomal localization of TLR4 and the activations of caspases, and (7) that the lentivirus-mediated knockdown of GNPAT, a rate-limiting enzyme of Pls synthesis, activated caspase-8 and caspase-3 in microglial cells, which suggested a possible mechanism of our previous finding that a reduction of cellular Pls could lead to the NF-κB activation [10].

It has been shown that TLR4 endocytosis is required for the downstream activation of TRIF-mediated type I interferons expression in mouse macrophages and Ba/F3 cells as a novel role in regulating innate immunity [15]. The LPS binding to

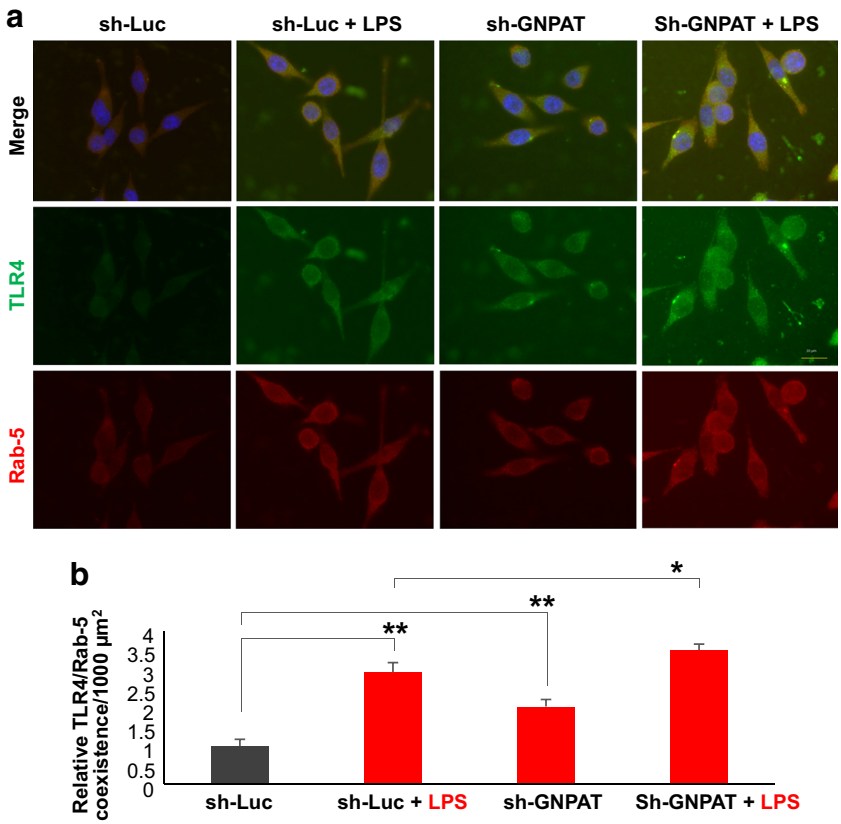


**Fig. 9** Knockdown of GNPAT accelerates the endocytosis of TLR4. **a** Immunocytochemistry study showed the co-expression of TLR4 and Rab5 in BV2 cells infected with the lentiviral particles delivering control sh-RNA (sh-Luc) and sh-RNA against GNPAT (sh-GNPAT) followed by the treatments with or without LPS (1 μg/ml) for 3 h. **b** The quantification of the image intensities of the TLR4 expression with the Rab5 examined by the hybrid cell count software (Keyence microscopy). The data represents the mean values and the error bars indicate S.E.M (*$P < 0.05$; **$P < 0.01$; $n = 5$)

TLR4 triggers the NF-κB activation, which is regulated by TIRAP and MyD88 adaptor proteins, then the TLR4 is internalized into the endosomes leading to the activation of a second signaling pathway triggering the interferon regulatory factor-3 (IRF-3) activation through the sorting adaptors, e.g., Toll/interleukin-1 receptor domain-containing adaptor inducing type I interferons-related adaptor molecule (TRAM) and TRIF [39]. Inhibition of the TLR4 endocytosis selectively inhibits TRAM and TRIF signaling in macrophages [15, 40]. As shown in BV2 cells (Fig. 4a), coexistence of TLR4 in the early endosomal protein Rab-5 was not detectable by the short-time (0.5 h) treatments of LPS but the internalization slowly increased thereafter reaching a steady-state level by 3 h LPS treatments. In addition, a dynamin blocker, dynasore, was able to reverse the LPS-induced TLR4 coexistence in the early endosome.

Endocytosis in eukaryotic cells is mainly classified into three categories: micropinocytosis, clathrin-dependent (CDE), and clathrin-independent endocytosis (CIE) [41, 42]. In the present study, we found that the LPS-induced internalization of TLR4 was dynamin-dependent and TLR4 was co-localized with an early endosomal marker, Rab-5. According to the characteristics of the CDE [41], it is likely that the endocytosis of TLR4 inducing signaling in the present study is mediated by the CDE. On the other hand, among the CIE, caveolin/lipid raft-mediated endocytosis (C/LR) has recently attracted an attention due to broad roles of lipid raft microdomains of the membrane in signal transduction. Interestingly, it has been shown that the CDE and C/LR have different roles in TLR4 signaling in macrophages; the CDE is necessary for inducing signaling, while the C/LR suppresses TLR4 signaling by accelerating degradation of TLR4 [20]. In addition to this functional difference, the C/LR endocytosis is shown to be devoid of classical early endosomal markers such as Rab-5 and early endosome antigen 1 [43]. In the present study, the pretreatment with sPls abolished the coexistence of TLR4 with Rab-5 and even decreased TLR4 immunoreactivity in the cytosol 3 h after LPS treatment (Fig. 8), which might be due to the degradation of TLR4 and need to be further studied to address this issue. Furthermore, we have found an increased expression of TLR4 after 3 h of the LPS treatments, and it could be due to the protein stability because we did not find any changes in the mRNA expression of TLR4. It has been shown that lipid rafts are enriched in Pls and the deficiency of Pls results in the impairment of lipid raft functions [35–37]. We showed that the breakdown of lipid raft function by depleting plasma membrane cholesterol with MβCD blocked the suppressing effect of Pls on the LPS-induced *IL-1β* expression. Furthermore, MβCD itself did not affect the LPS-induced cytokine expression (Fig. S2), indicating that TLR4 signaling induced by the dynamin-mediated endocytosis was not associated with lipid rafts. These findings, taken together, suggest that Pls may be involved in the C/LR and the pretreatment with Pls may not simply inhibit the LPS-induced

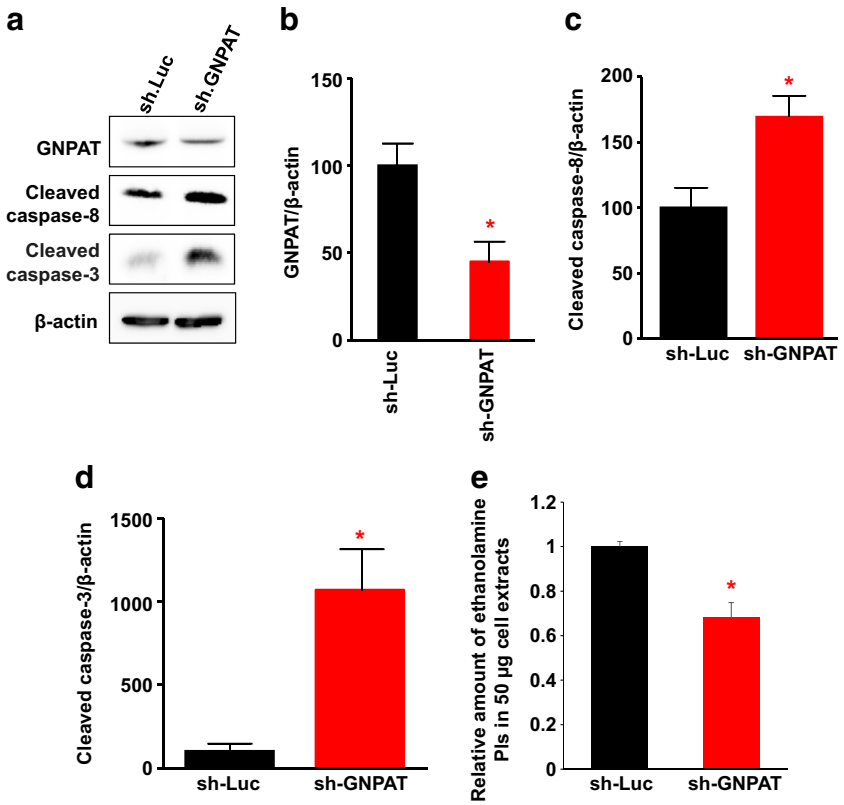


**Fig. 10** Knockdown of GNPAT activates caspase-8 and caspase-3 in BV2 cells. **a** Representative Western blot data showed an increase in cleaved caspase-8 and caspase-3 in BV2 cells by knockdown of GNPAT using sh-RNA for 72 h. **b**-**d** Quantification data of the Western blotting assays showed a significant reduction of GNPAT (**b**), cleaved caspase-8 (**c**) and cleaved caspase-3 (**d**) proteins by the knockdown of GNPAT gene in BV2 cells. **e** LC-MS data showed a decrease in total ethanolamine Pls by the GNPAT knockdown in the BV2 cells. (*$P < 0.05$, Student's *t* test, $n = 3$)

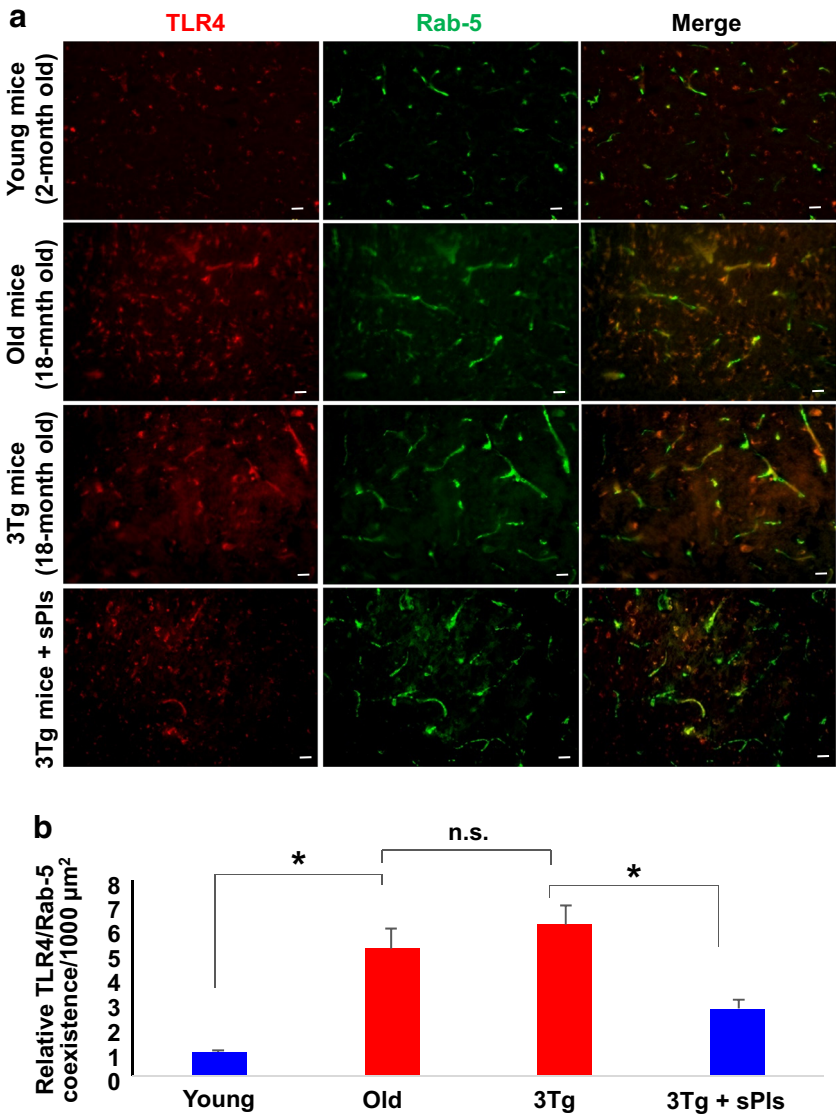


**Fig. 11** Endocytosis of TLR4 is enhanced in aged mice and AD model mice. **a** IHC studies showed the TLR4 (red) and Rab5 (green) staining of the brain cortex of young mice (2-month old B6 mice), old mice (18-month old B6), control 3Tg mice (18-month old triple transgenic), and the 18-month old 3Tg mice subjected to sPls drinking (0.1 µg/ml) for 15 months. **b** The quantification data of panel (**a**) showed the TLR4 stained area overlapped in the Rab5 stained area of the cells. The analysis was performed with three brain slices of each mice cortex and each group contained five individual mice ($n = 5$; $^{*}P < 0.05$; $^{**}P < 0.01$; n.s., non-significant). The data was represented as mean ± S.E.M.

CDE but also enhance the C/LR to degrade TLR4, thereby suppressing TLR4 signaling. On the other hand, the knockdown of Pls synthesizing enzyme, GNPAT, which was shown to reduce Pls content in microglia and induce microglial activation [10], activated caspase-8 and caspase-3 (Fig. 10). This might be due to the downregulation of C/LR endocytosis resulting in the relative activation of the CDE to induce TLR4 signaling.

We have previously shown that the systemic LPS-induced neuroinflammatory responses, such as glial activation and cytokines expression in the mouse prefrontal cortex and hippocampus were attenuated by co-administration of Pls [13]. Our present findings suggest that a possible mechanism of the anti-inflammatory action of Pls upon LPS stimulation is due to the inhibition of the CDE-dependent internalization of TLR4 and the enhancement of the C/LR-mediated degradation of TLR4. The depletion of Pls in rhizomelic chondrodysplasia punctata (RCDP) patients shows decreased number of caveolae but increased clathrin concentration in the plasma membrane suggesting that C/LR endocytic uptake is reduced in Pls-deficient human skin fibroblast cells [37]. Our results also suggest that Pls can influence the LPS-induced C/LR in microglial cells.

Importantly, we found that the dynamin-mediated endocytosis was an early event for the mouse microglial activation by LPS. Our results further showed that the dynamin blocker was able to reverse the inflammatory effects of LPS including the activation of caspase-3. Caspase-3 has been newly recognized as a key molecule responsible for the rate-limiting step of inflammation and is activated among microglia cells in the frontal cortex of the AD brains [26]. The dynamin-mediated internalization of TLR4 in the AD brain was mostly elusive. We, for the first time, report that there is an increased endocytosis of TLR4 not only in the aged mice brain but also in the AD model mice brain. These increased TLR endocytosis might be a key event for the neurodegeneration signaling in the brain, which may directly linked to the reduction of brain

Pls. This is further suggested by our previous findings that a reduction of brain Pls in aged and AD model mice [27]. Our present results, together with our previous studies [10, 13], suggest that Pls inhibit the major inflammatory processes, such as caspase activation and nuclear localization of p65 protein, in microglial cells of murine brain by regulating the TLR4 internalization. Further study will be necessary to elucidate the direct role of Pls in the CDE and C/LR-mediated TLR4 internalization in the microglial cells. This may explain why a reduction of brain Pls, which is common in the AD brain [8-10], can trigger the neuroinflammatory responses including the activation of caspases and NF-κB. Furthermore, our present findings can also suggest a possible mechanism of sPls-mediated cognition improvement, which was reported among mild AD patients [28].

**Acknowledgements** We appreciate the technical assistance of the Research Support Center, Graduate School of Medical Sciences, Kyushu University. We thank Dr. A. Ibrahim for insightful discussion and suggestions to continue this study. We appreciate the technical assistance from Ayako Tajima to perform experiments.

**Funding Information** This work was supported by JSPS KAKENHI grant number 26460320 to Toshihiko Katafuchi, JSPS Wakate B (16K19007) to MSH and Egyptian ministry of higher education scholarship for young scientist fellowship to F. Ali.

**Abbreviations** AD, Alzheimer's disease; ANOVA, one-way analysis of variance; BCA, bicinchoninic acid; BSA, bovine serum albumin; CDE, clathrin-dependent endocytic; CHO, Chinese hamster ovary; CIE, clathrin-independent endocytic; C/LR, caveolin/lipid raft-mediated endocytic; DAPI, 4′,6-diamidino-2-phenylindole; DEVD, Z-DEVD-fmk; DMEM, Dulbecco's modified Eagle medium; FBS, fetal bovine serum; GAPDH, glyceraldehyde-3-phosphae dehydrogenase; GNPAT, glycerone phosphate O-acyltransferase; HEK, human embryonic kidney; IL-1β, interleukin-1β; IL-1R, interleukin-I receptor; IRF, interferon regulatory factor-3; LPS, lipopolysaccharide; MβCD, methyl-β-cyclodextrin; NF-κB, nuclear factor-κB; PARP1, polyadenosine diphosphate ribosepolymerase1; PBS, phosphate-buffered saline; PCR, polymerase chain reaction; Pls, plasmalogens; Pls-Etn, ethanolamine plasmalogens; RCDP, rhizomelic chondrodysplasia punctate; RIPA, radio-immunoprecipitation assay; SDS-PAGE, sodium dodecyl sulfate–polyacrylamide gel electrophoresis; sh-RNA, short hairpin-RNA; TBS, Tris-buffered saline; TDU, transduction unites; TIRAP, Toll/IL-1R domain-containing adaptor protein; TLR4, toll-like receptor 4; TNF-α, tumor necrosis factor-α; TRAM, Toll/interleukin-1 receptor domain-containing adaptor inducing type I interferons-related adaptor molecule; TRIF, Toll/interleukin-1 receptor domain-containing adaptor inducing type I interferons; VAD, Z-VAD-fmk

## References

1. Tanzi RE, Bertram L (2005) Twenty years of the Alzheimer's disease amyloid hypothesis: a genetic perspective. Cell 120(4):545–555. https://doi.org/10.1016/j.cell.2005.02.008
2. Haass C, Selkoe DJ (2007) Soluble protein oligomers in neurodegeneration: lessons from the Alzheimer's amyloid beta-peptide. Nat Rev Mol Cell Biol 8(2):101–112. https://doi.org/10.1038/nrm2101
3. Tahara K, Kim HD, Jin JJ, Maxwell JA, Li L, Fukuchi K (2006) Role of toll-like receptor signalling in Abeta uptake and clearance. Brain 129(Pt 11):3006–3019. https://doi.org/10.1093/brain/awl249
4. Apelt J, Schliebs R (2001) Beta-amyloid-induced glial expression of both pro- and anti-inflammatory cytokines in cerebral cortex of aged transgenic Tg2576 mice with Alzheimer plaque pathology. Brain Res 894(1):21–30
5. Salminen A, Ojala J, Suuronen T, Kaarniranta K, Kauppinen A (2008) Amyloid-beta oligomers set fire to inflammasomes and induce Alzheimer's pathology. J Cell Mol Med 12(6A):2255–2262. https://doi.org/10.1111/j.1582-4934.2008.00496.x
6. Fahy E, Subramaniam S, Brown HA, Glass CK, Merrill AH Jr, Murphy RC, Raetz CR, Russell DW et al (2005) A comprehensive classification system for lipids. J Lipid Res 46(5):839–861. https://doi.org/10.1194/jlr.E400004-JLR200
7. Maeba R, Ueta N (2003) Ethanolamine plasmalogens prevent the oxidation of cholesterol by reducing the oxidizability of cholesterol in phospholipid bilayers. J Lipid Res 44(1):164–171
8. Guan Z, Wang Y, Cairns NJ, Lantos PL, Dallner G, Sindelar PJ (1999) Decrease and structural modifications of phosphatidylethanolamine plasmalogen in the brain with Alzheimer disease. J Neuropathol Exp Neurol 58(7):740–747
9. Han X, Holtzman DM, McKeel DW Jr (2001) Plasmalogen deficiency in early Alzheimer's disease subjects and in animal models: molecular characterization using electrospray ionization mass spectrometry. J Neurochem 77(4):1168–1180
10. Hossain MS, Abe Y, Ali F, Youssef M, Honsho M, Fujiki Y, Katafuchi T (2017) Reduction of ether-type glycerophospholipids, plasmalogens, by NF-κB signal leading to microglial activation. J Neurosci 37(15):4074–4092. https://doi.org/10.1523/JNEUROSCI.3941-15.2017
11. Wood PL, Mankidy R, Ritchie S, Heath D, Wood JA, Flax J, Goodenowe DB (2010) Circulating plasmalogen levels and Alzheimer disease assessment scale-cognitive scores in Alzheimer patients. J Psychiatry Neurosci 35(1):59–62
12. Hossain MS, Ifuku M, Take S, Kawamura J, Miake K, Katafuchi T (2013) Plasmalogens rescue neuronal cell death through an activation of AKT and ERK survival signaling. PLoS One 8(12):e83508. https://doi.org/10.1371/journal.pone.0083508
13. Ifuku M, Katafuchi T, Mawatari S, Noda M, Miake K, Sugiyama M, Fujino T (2012) Anti-inflammatory/anti-amyloidogenic effects of plasmalogens in lipopolysaccharide-induced neuroinflammation in adult mice. J Neuroinflammation 9:197. https://doi.org/10.1186/1742-2094-9-197
14. Akira S, Takeda K (2004) Functions of toll-like receptors: lessons from KO mice. C R Biol 327(6):581–589
15. Kagan JC, Su T, Horng T, Chow A, Akira S, Medzhitov R (2008) TRAM couples endocytosis of Toll-like receptor 4 to the induction of interferon-β. Nat Immunol 9(4):361–368. https://doi.org/10.1038/ni1569
16. Wong SW, Kwon MJ, Choi AM, Kim HP, Nakahira K, Hwang DH (2009) Fatty acids modulate toll-like receptor 4 activation through regulation of receptor dimerization and recruitment into lipid rafts in a reactive oxygen species-dependent manner. J Biol Chem 284(40):27384–27392. https://doi.org/10.1074/jbc.M109.044065
17. Husebye H, Halaas O, Stenmark H, Tunheim G, Sandanger O, Bogen B, Brech A, Latz E et al (2006) Endocytic pathways regulate Toll-like receptor 4 signaling and link innate and adaptive immunity. EMBO J 25(4):683–692. https://doi.org/10.1038/sj.emboj.7600991
18. Shuto T, Kato K, Mori Y, Viriyakosol S, Oba M, Furuta T, Okiyoneda T, Arima H et al (2005) Membrane-anchored CD14 is required for LPS-induced TLR4 endocytosis in TLR4/MD-2/CD14 overexpressing CHO cells. Biochem Biophys Res Commun 338(3):1402–1409. https://doi.org/10.1016/j.bbrc.2005.10.102

19. Pascual-Lucas M, Fernandez-Lizarbe S, Montesinos J, Guerri C (2014) LPS or ethanol triggers clathrin- and rafts/caveolae-dependent endocytosis of TLR4 in cortical astrocytes. J Neurochem 129(3):448–462. https://doi.org/10.1111/jnc.12639
20. Cai W, Du A, Feng K, Zhao X, Qian L, Ostrom RS, Xu C (2013) Adenylyl cyclase 6 activation negatively regulates TLR4 signaling through lipid raft-mediated endocytosis. J Immunol 191 (12):6093-6100. doi:https://doi.org/10.4049/jimmunol.1301912
21. Budihardjo I, Oliver H, Lutter M, Luo X, Wang X (1999) Biochemical pathways of caspase activation during apoptosis. Annu Rev Cell Dev Biol 15:269–290. https://doi.org/10.1146/annurev.cellbio.15.1.269
22. Wu X, Guo R, Chen P, Wang Q, Cunningham PN (2009) TNF induces caspase-dependent inflammation in renal endothelial cells through a Rho- and myosin light chain kinase-dependent mechanism. Am J Physiol Renal Physiol 297(2):F316–F326. https://doi.org/10.1152/ajprenal.00089.2009
23. Su JH, Zhao M, Anderson AJ, Srinivasan A, Cotman CW (2001) Activated caspase-3 expression in Alzheimer's and aged control brain: correlation with Alzheimer pathology. Brain Res 898(2): 350–357
24. D'Amelio M, Cavallucci V, Middei S, Marchetti C, Pacioni S, Ferri A, Diamantini A, De Zio D et al (2011) Caspase-3 triggers early synaptic dysfunction in a mouse model of Alzheimer's disease. Nat Neurosci 14(1):69–76. https://doi.org/10.1038/nn.2709
25. Stone JR, Okonkwo DO, Singleton RH, Mutlu LK, Helm GA, Povlishock JT (2002) Caspase-3-mediated cleavage of amyloid precursor protein and formation of amyloid β peptide in traumatic axonal injury. J Neurotrauma 19(5):601–614. https://doi.org/10.1089/089771502753754073
26. Burguillos MA, Deierborg T, Kavanagh E, Persson A, Hajji N, Garcia-Quintanilla A, Cano J, Brundin P et al (2011) Caspase signalling controls microglia activation and neurotoxicity. Nature 472(7343):319–324. https://doi.org/10.1038/nature09788
27. Hossain MS, Abe Y, Ali F, Youssef M, Honsho M, Fujiki Y, Katafuchi T (2017) Reduction of ether-type glycerophospholipids, plasmalogens, by NF-kappaB signal leading to microglial activation. J Neurosci 37(15):4074–4092. https://doi.org/10.1523/JNEUROSCI.3941-15.2017
28. Fujino T, Yamada T, Asada T, Tsuboi Y, Wakana C, Mawatari S, Kono S (2017) Efficacy and blood plasmalogen changes by oral administration of plasmalogen in patients with mild Alzheimer's disease and mild cognitive impairment: a multicenter, randomized, double-blind, placebo-controlled trial. EBioMedicine 17:199–205. https://doi.org/10.1016/j.ebiom.2017.02.012
29. Mawatari S, Yunoki K, Sugiyama M, Fujino T (2009) Simultaneous preparation of purified plasmalogens and sphingomyelin in human erythrocytes with phospholipase A1 from Aspergillus orizae. Biosci Biotechnol Biochem 73(12):2621–2625. https://doi.org/10.1271/bbb.90455
30. Braverman NE, Moser AB (2012) Functions of plasmalogen lipids in health and disease. Biochim Biophys Acta 1822(9):1442–1452. https://doi.org/10.1016/j.bbadis.2012.05.008
31. Oettinghaus B, Schulz JM, Restelli LM, Licci M, Savoia C, Schmidt A, Schmitt K, Grimm A et al (2016) Synaptic dysfunction, memory deficits and hippocampal atrophy due to ablation of mitochondrial fission in adult forebrain neurons. Cell Death Differ 23(1):18–28. https://doi.org/10.1038/cdd.2015.39
32. Ifuku M, Hossain SM, Noda M, Katafuchi T (2014) Induction of interleukin-1β by activated microglia is a prerequisite for immunologically induced fatigue. Eur J Neurosci 40(8):3253–3263. https://doi.org/10.1111/ejn.12668
33. Cohen GM (1997) Caspases: the executioners of apoptosis. Biochem J 326(Pt 1):1–16
34. Schmitz ML, Baeuerle PA (1991) The p65 subunit is responsible for the strong transcription activating potential of NF-κB. EMBO J 10(12):3805–3817
35. Pike LJ, Han X, Chung KN, Gross RW (2002) Lipid rafts are enriched in arachidonic acid and plasmenylethanolamine and their composition is independent of caveolin-1 expression: a quantitative electrospray ionization/mass spectrometric analysis. Biochemistry 41(6):2075–2088
36. Rodemer C, Thai TP, Brugger B, Kaercher T, Werner H, Nave KA, Wieland F, Gorgas K et al (2003) Inactivation of ether lipid biosynthesis causes male infertility, defects in eye development and optic nerve hypoplasia in mice. Hum Mol Genet 12(15):1881–1895
37. Thai TP, Rodemer C, Jauch A, Hunziker A, Moser A, Gorgas K, Just WW (2001) Impaired membrane traffic in defective ether lipid biosynthesis. Hum Mol Genet 10(2):127–136
38. Wanders RJ, Waterham HR (2005) Peroxisomal disorders I: biochemistry and genetics of peroxisome biogenesis disorders. Clin Genet 67(2):107–133. https://doi.org/10.1111/j.1399-0004.2004.00329.x
39. Kagan JC, Medzhitov R (2006) Phosphoinositide-mediated adaptor recruitment controls Toll-like receptor signaling. Cell 125(5):943–955. https://doi.org/10.1016/j.cell.2006.03.047
40. Tanimura N, Saitoh S, Matsumoto F, Akashi-Takamura S, Miyake K (2008) Roles for LPS-dependent interaction and relocation of TLR4 and TRAM in TRIF-signaling. Biochem Biophys Res Commun 368(1):94–99. https://doi.org/10.1016/j.bbrc.2008.01.061
41. Doherty GJ, McMahon HT (2009) Mechanisms of endocytosis. Annu Rev Biochem 78:857–902. https://doi.org/10.1146/annurev.biochem.78.081307.110540
42. Grant BD, Donaldson JG (2009) Pathways and mechanisms of endocytic recycling. Nat Rev Mol Cell Biol 10(9):597–608. https://doi.org/10.1038/nrm2755
43. Nichols BJ (2002) A distinct class of endosome mediates clathrin-independent endocytosis to the Golgi complex. Nat Cell Biol 4(5): 374–378. https://doi.org/10.1038/ncb787